# Unconventional Route to High-Pressure and -Temperature Synthesis of GeSn Solid Solutions

# Unconventional route to high pressure and temperature synthesis of GeSn solid solutions

George Serghiou,* Nicholas Odling, Hans Josef Reichmann, Kristina Spektor, Wilson A. Crichton, Gaston Garbarino, Mohamed Mezouar and Anna Pakhomova

**ABSTRACT:** Ge and Sn are unreactive at ambient conditions. Their significant promise for optoelectronic applications is thus largely confined to thin film investigations. We sought to remove barriers to reactivity here by accessing a unique pressure, 10 GPa, where the two elements can adopt the same crystal structure (tetragonal - $I4_1/amd$) and exhibit compatible atomic radii. The route to GeSn solid solution however, even under these directed conditions, is different. Reaction upon heating at 10 GPa occurs between unlike crystal structures (Ge - $Fd\bar{3}m$ and Sn - $I4/mmm$) which also have highly incompatible atomic radii. They should not react, but they do. A reconstructive transformation of $I4/mmm$ into the $I4_1/amd$ solid solution then follows. The new tetragonal GeSn solid solution ($I4_1/amd$ a = 5.280 (1) Å, c = 2.915 (1) Å, Z = 4 at 9.9 GPa and 298 K) also constitutes the structural and electronic bridge between four-fold and newly prepared eight-fold coordinated alloy cubic symmetries. Furthermore, using this high pressure route, bulk cubic diamond-structured GeSn alloys, can now be obtained at ambient pressure. The findings here remove confining conventional criteria on routes to synthesis. This opens innovative avenues to advanced materials development.

There is a strong long-standing drive to extend the functionality of (Si, Ge)-based technology from microelectronics into optoelectronics.[1] The indirect band-gap of the cubic diamond-structured Si, Ge and SiGe solid solutions makes this problematic.[2-4] Solid solution of Ge with Sn however, can lead to direct band-gap formation which is thus being intensely investigated.[5-8] These investigations however, are largely limited to thin films because Ge and Sn are unreactive at ambient pressure due to their dissimilar crystal and electronic structures and markedly different atomic radii.[9,10] Pressure however, can have a profound effect on structural and electronic phase relations and therefore on reactivity[11-13] leading also above 10 GPa to synthesis of a new cubic eightfold coordinated GeSn solid solution.[14] At 10 GPa, a region of the phase diagram can be accessed where Ge and Sn may have the same crystal structure and favourable atomic radii ratios for solid solution formation.[11,15] We describe the endmember Ge and Sn phase relations here and investigate the special region where the intention is to have the two endmembers have the same crystal structure and compatible atomic radii. At between ambient and 10 GPa, Ge adopts the cubic $Fd\bar{3}m$ (c-Ge) structure whereas Sn adopts a tetragonal $I4_1/amd$ structure (β-Sn, Strukturbericht Designation A5). At 10 GPa cubic Ge also transforms to the $I4_1/amd$ structure (β-Ge). Sn, on other hand, transforms above 10 GPa to another tetragonal phase with $I4/mmm$ space group (t-Sn).[16] The only pressure where Ge and Sn are compatible according to the Hume-Rothery criteria[17], is at 10 GPa. In particular, at 10 GPa Ge and Sn can uniquely adopt the same crystal structure, $I4_1/amd$, and have atomic radii that differ by 11%[18] well below the Hume-Rothery 15%[17] tolerance threshold for solid solution formation.

To investigate this region for creating reactivity to make a bulk Ge-Sn alloy we employed a multi-anvil large volume press coupled with requisite and detailed *in-situ* angle dispersive monochromatic synchrotron X-ray diffraction measurements.[18] The starting mixture was a 60:40 at% c-Ge and β-Sn mixture which was then compressed to 9.9 GPa. At 9.9 GPa however, conversion to β-Ge has not occurred. Upon heating β-Ge also does not appear (Figure 1a, c, Figure S2). This phase transition is severely kinetically hindered. Sn at 9.9 GPa is in the β-Sn structure with only a weak t-Sn presence (Figure 1a, c, Figure S2). Upon heating, the presence of t-Sn becomes more notable at 327 K, accompanied by c-Ge. At 352 K t-Sn is the principal Sn phase present and by 384 K any residual β-Sn has disappeared with c-Ge being the only Ge phase present. The first noticeable signs of a surprising reaction between c-Ge and t-Sn occur above 384 K. In particular between 298 K and 384 K the (110) diffraction peak of t-Sn (black arrow at 489 K) shifts as normal to lower angles, due to thermal expansion (Figure 1a, c, Figure S2). It does so by 0.009 degrees. Between 384 K and 489 K, however, this peak unexpectedly shifts to higher angle by 0.006 degrees due to uptake of smaller Ge by t-Sn (Figure 1a, c, Figure S2). Between 489 K and 532 K the (110) peak shifts to higher angle by a further 0.006 degrees. But above 489 K concomitant with the additional Ge uptake in t-Sn, diffraction peaks of β-GeSn emerge and the $Fd\bar{3}m$ and I4/mmm peaks decline in intensity. Between 556 K and 604 K the only sample diffraction peaks present are those corresponding to the new β-GeSn solid solution, but they are broad and diffuse. This indicates structural disorder

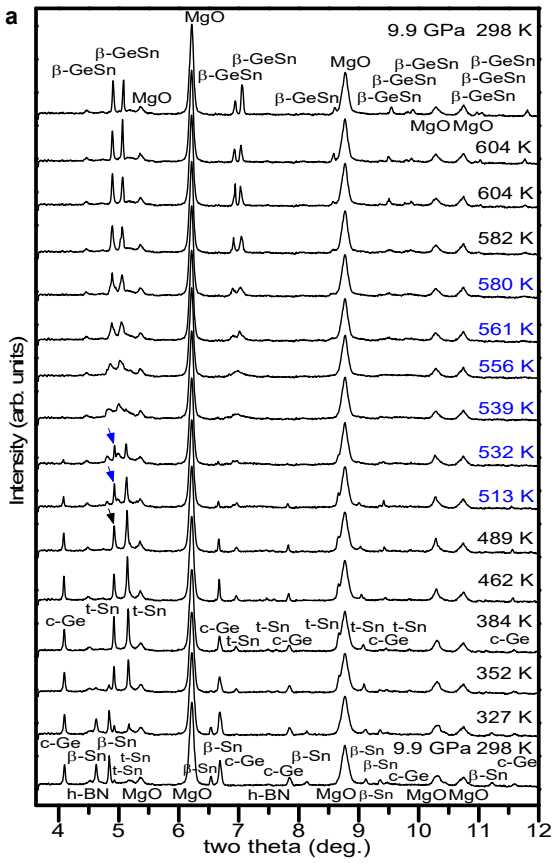


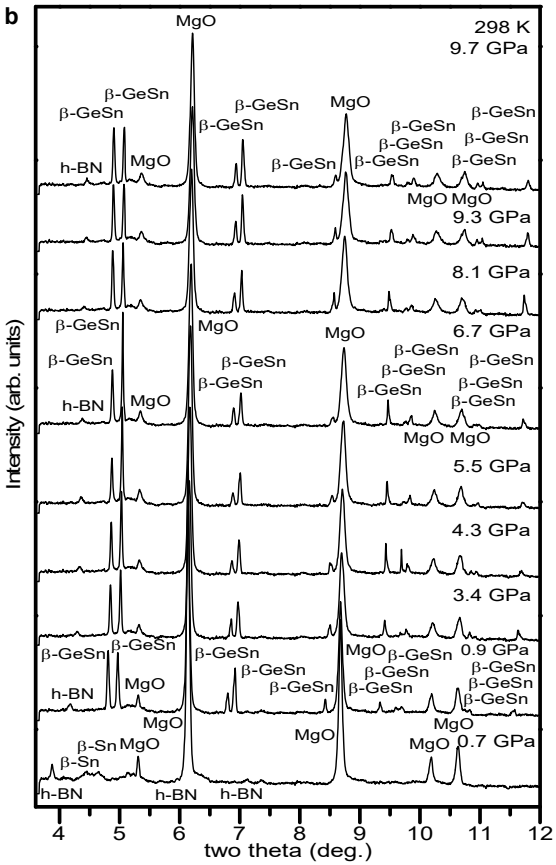


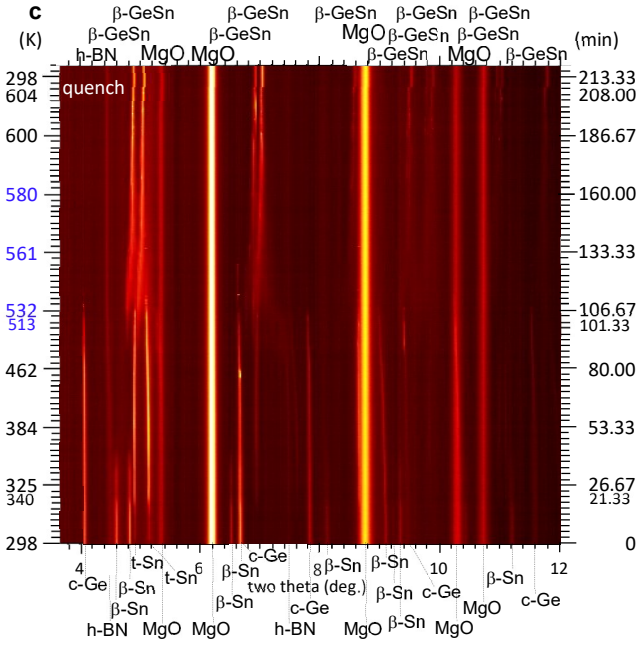


**Figure 1.** (a) Angle-dispersive X-ray diffraction patterns upon heating a c-Ge and t-Sn mixture (from a 60:40 starting mix) at 9.9 GPa in a multi-anvil device and formation of a β-GeSn solid solution upon heating {a = 5.294 (1) Å, c = 2.926 (1) Å at 9.9 GPa and 604K (Figure S3 including Le Bail fitting)}.[18] A Vegards law assessment[18] indicates a β-$Ge_{0.44}Sn_{0.56}$ composition upon temperature quenching {a = 5.280 (1) Å, c = 2.915 (1) Å at 9. 9 GPa and 298 K (Figures S4 including Le Bail fitting)}.[18] Error assessments in pressure and temperature measurement are provided in the supporting information[18].The supplementary information[18] also includes a more detailed plot containing 31 diffraction patterns upon heating (Figure S2). The black arrow pinpoints the t-Sn diffraction peak ((110) plane) at a temperature where this peak is continuing to shift to higher angles (and hence Ge uptake is continuing) but before β-GeSn appears. The blue arrows in the ensuing two patterns (at 513 K and 532 K) designate the continued shifting to the right of this peak, and the concurrent emergence of β-GeSn solid solutions and decline of the c-Ge and t-Sn patterns. The temperatures in blue designate the region throughout which the structural reconstruction (from $I4/mmm$ to $I4_1/amd$) and significant compositional changes occur in solid solution. The plot in the supplementary information[18] shows this transitional region in much greater detail (Figure S2). (b) Patterns were collected on decompression. The solid solution is stable down to 0.9 GPa, with a broadened β-Sn pattern detected at 0.7 GPa (Figures S5-S12 including Le Bail whole pattern fittings are shown in the supplementary information).[18] (c) Time – temperature - intensity - two theta plot at 9.9 GPa in the solid state and upon temperature quenching. The left horizontal bars are not scales, but references to correlate times on the right vertical axis with their corresponding temperatures on the left vertical axis. The blue - coloured temperatures designate the region where the structural reconstruction (from $I4/mmm$ to $I4_1/amd$) and significant compositional changes occur in the new solid solution.

and compositional diversity, that is a range of β-GeSn compositions. The peaks are also shifting to higher angles and gradually become more pronounced with temperature. This region hence indicates considerable restructuring as well as convergence on an overall higher Ge containing β-GeSn phase. At 582 K the β-GeSn peaks are stronger and sharper and continue to gradually improve up to the highest annealing temperature of 604 K (Figure 1a, Figure S2-S3). From 582 K to 604 K, the β-GeSn peaks no longer significantly shift to higher angles. This is because a more limited shift to higher angles is compensated by a comparable shift to lower angles due to thermal expansion. The contribution of thermal expansion alone to β-GeSn peak shifting to lower angles is evident from the significant peak shifting to higher angles on temperature quenching (Figure 1a, c, Figure S2-S4). Using a Vegards law estimation, the composition of the new tetragonal solid solution is β-$Ge_{0.44}Sn_{0.56}$ at 9.9 GPa and 298 K (Figure S4).[18] Since the β-solid solution has the same space group as β-Sn and unit cell parameters between those of the endmembers, it is reasonable to assume that all the atoms are on the high-symmetry Wyckoff 4a position. Upon decompression the new tetragonal solid solution is retained down to 0.9 GPa (Figure 1b, Figures S5-S12). At 0.9 GPa a notable shoulder is also present on the left of the (011) peak (near 5 degrees), which is a harbinger of significant Sn exsolution (Figure 1b). Accordingly, β-Sn peaks are observed on complete decompression accompanied by a nanocrystalline c-$Ge_{0.68}Sn_{0.32}$ pattern (Figure 2, Figure S13).[18] The nanocrystalline cubic diamond-structured crystallite size is evaluated to be about 7 nm.[18,19]

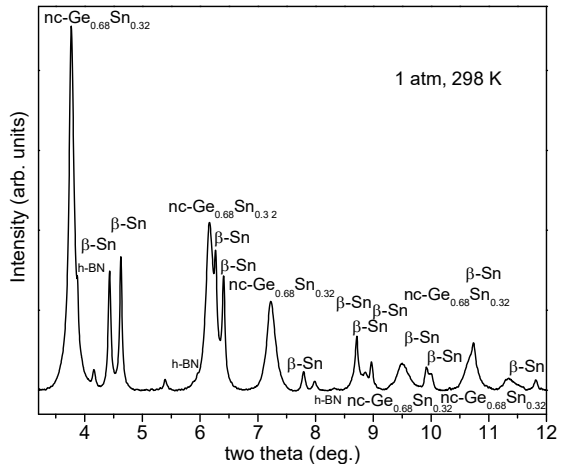


**Figure 2.** Nanocrystalline cubic diamond-structured phase with composition $Ge_{0.68}Sn_{0.32}$ based on a Vegards law estimation[18], together with β-Sn are recovered upon complete release of pressure {$Fd\bar{3}m$, a = 5.925 (1) Å, at 1 atm and 298 K, nanocrystalline size: 6.5 nm, (Figure S13 including Le Bail whole pattern fitting)}.[18]

With the barriers to reactivity removed, allowing formation of the new tetragonal solid solution phase, we now consider the unusual route to its synthesis. We then describe how this new phase made possible by this unusual route plays a pivotal role in markedly expanding the group IVA materials landscape[14]. According to the Hume-Rothery criteria c-Ge and t-Sn are incompatible structurally and electronically for solid solution formation. They have unlike crystal structures, their atomic radii differ by a substantial 24%, well above the 15% tolerance ratio, c-Ge is a $sp^3$ hybridized semiconductor whereas t-Sn is a sp de-hybridized metal[16-25] (supplementary information).[18] With these characteristics, they should not react. But they do. Ge diffuses into the t-Sn structure as seen by the shift to higher angles of the t-Sn (110) peak pinpointed by black and blue arrows (Figure 1a). This peak initially shifts to the left like the others (Figure 1a, Figure S2). Unlike the other peaks (and this one for pure t-Sn) which continue to shift to the left upon further heating, this one unexpectedly here then shifts to the right throughout the 384 K to 532 K temperature regime (Figure 1a, Figure S2). Annealing and raising the temperature further, cannot promote any additional Ge incorporation into t-Sn. This now is not surprising, given the substantial Ge and Sn incompatibility which causes strain in the t-Sn lattice with Ge incorporated. The strained t-$SnGe_x$ lattice however has an opportunity at 10 GPa. It can remove this strain and incorporate more of the surrounding abundant c-Ge ($Fd\bar{3}m$). It can do this by transforming from $I4/mmm$ to a favourable crystal structure, accessible for both elements at this specific pressure, $I4_1/amd$[11,15,16], at the expense of the $Fd\bar{3}m$ and $I4/mmm$ phases. The $I4/mmm$ to $I4_1/amd$ transformation is however reconstructive.[24] This account is consistent with the evolution of the diffraction patterns (Figure 1a, c, Figure S2). Once the apparent limit is approached on Ge incorporation in t-Sn at 489 K, an $I4_1/amd$ broadened pattern with evolving peak shape profile emerges and gradually improves within a significant structural and compositional transition zone between 536 K and 582 K (Figure1a, c, Figure S2).[18] There is the additional question however, of why would t-Sn accept any Ge to begin with, given their significant incompatibility with respect to the Hume-Rothery criteria? This may be traced back to the extremely favourable relative specific volume of β-GeSn with respect to t-Sn and c-Ge (supplementary information).[18] In particular, from the specific volume point of view, there is no composition which would favour the reactants, t-Sn and c-Ge over the product, β-GeSn. While this is not a sufficient criterion, it may provide a driving force for incorporation of enough Ge to trigger restructuring to the favourable $I4_1/amd$ phase. Notably this process would also hold true for β-Ge and t-Sn starting materials because their atomic radii ratios are also incompatible at 18%[18]. The new solid solution structure is stable upon temperature quenching and almost down to ambient pressure. At ambient pressure another significant transformation occurs to nanocrystalline diamond-structured nc-$Ge_{0.68}Sn_{0.32}$ together with β-Sn (Figure 2, Figure S13). The Ge-rich cubic diamond-structured phase evidently results from ex-solution of β-Sn from the β-GeSn solid solution producing a Ge-richer composition, stable at ambient conditions in the nanocrystalline cubic diamond-structured phase.

These results are a fountainhead for developing new materials landscapes in the crystal chemically and techno-

logically pivotal, from ceramic to semiconducting solid solution domain.[26,27] Here, the new β-GeSn phase, with its mixed covalent and metallic bonding and six-fold coordination, is also the structural and electronic bridge between the four-fold coordinated cubic diamond-structured and new frontier eight-fold coordinated body-centered cubic (bcc) Ge-Sn alloys[14]. With creation of this bridge, synthesis of the new bcc alloys is no longer, because of the incompatibility of Ge and Sn, limited to multi-phase Ge and Sn starting mixtures. Now β-GeSn alloys will be used as a single phase synthetic vehicle for preparing eightfold coordinated cubic alloys. This will allow us to closely investigate cubic alloy composition as well as crystal quality and stability formed from a known single phase starting composition, as compared to synthesis from endmember physical mixtures.

The β-GeSn bridge is already a synthetic vehicle on its low pressure side in making here bulk nanocrystalline cubic diamond-structured Ge-Sn, a hotly investigated system for optoelectronics, confined previously to thin films.[5-8] Through this work, investigation of bulk versus thin films can be examined together with the effect of crystal size and composition on direct band-gap formation. Moreover, we are also pursuing high pressure and temperature synthesis of ternary (Ge-Sn-Si) systems. These can offer additional tunability[28] and entropic stabilization.[29,30] Stabilization may be further enhanced by low temperature decompression leading to complete recovery of novel Ge-rich octahedrally coordinated alloys with intriguing electronic, optical and structural properties.[31]

## ASSOCIATED CONTENT

**Supporting Information**

The supporting information has 6 sections, and associated figures S1-S14 on (i) experimental procedures, (ii) atomic radii calculations, (iii) specific volume and Vegards law calculations (iv) detailed β-GeSn formation patterns, (v) Le Bail fits and crystallographic data of experimental diffraction patterns, (vi) further recovered Ge-Sn pattern and (vii) structural schematics. This material is available free of charge via the Internet at http://pubs.acs.org.

## AUTHOR INFORMATION


### Corresponding Author

George Serghiou – University of Edinburgh, School of Engineering, Sanderson Building, Kings Buildings, Robert Stevenson Road EH9 3FB, Scotland, United Kingdom
orcid.org/0000-0002-5471-1735;
Email: george.serghiou@ed.ac.uk

### Authors

Nicholas Odling - University of Edinburgh, School of Geosciences, The Grant Institute, Kings Buildings, West Mains Road, EH9 3JW UK

Hans Josef Reichmann - Deutsches GeoForschungsZentrum GFZ Telegrafenberg, 14473 Potsdam Germany

Kristina Spektor - ESRF The European Synchrotron, 71 avenue des Martyrs, 38000 Grenoble France

Wilson A. Crichton - ESRF The European Synchrotron, 71 avenue des Martyrs, 38000 Grenoble France

Gaston Garbarino - ESRF The European Synchrotron, 71 avenue des Martyrs, 38000 Grenoble France

Mohamed Mezouar - ESRF The European Synchrotron, 71 avenue des Martyrs, 38000 Grenoble France

Anna Pakhomova - Deutsches Elektronen-Synchrotron (DESY), 22607, Hamburg, Germany


## ACKNOWLEDGMENTS


Parts of this research were carried out at ID06 and ID27 at the European Synchrotron Radiation Facility (ESRF) in the context of CH5596 and CH5448. Parts of this research were also carried out at P02.2/PETRA at the German Electron Synchrotron (DESY), a member of the Helmholtz Association (HGF) in the context of DESY-D-I-20160758. We gratefully thank both institutions for their support. We also thank Mike Hall, Fraser Christensen, Euan Flett, Reik Suenkel and Andreas Ebert for contributing to component micromanufacture, assembly and characterization and Laurence Nigay for incisive comments on the manuscript.


## REFERENCES


(1) Schilz, J.; Romanenko, V. N. Bulk growth of silicon-germanium solid solutions J. Mat. Sci. Mat. in Electr. **1995**, 6, 265-279.

(2) Hybertsen, M. S.; Louie, S. G. Electron correlation in semiconductors and insulators – band-gaps and quasi-particle energies. *Phys. Rev. B* **1986,** 34, 5390–5413.

(3) Braunstein, R.; Moore, A. R.; Herman, F. Intrinsic optical absorption in germanium-silicon alloys. *Phys. Rev. B* **1958,** 109, 695–710.

(4) Serghiou, G.; Ji, G.; Koch-Müller, M.; Odling, N.; Reichmann, H.-J.; Wright, J. P.; Johnson, P. Dense $Si_xGe_{1-x}$ (0 <x< 1) Materials Landscape Using Extreme Conditions and Precession Electron Diffraction. *Inorg. Chem.* **2014,** 53, 5656-5662.

(5) Wirths, S.; Geiger, R.; von den Driesch, N.; Mussler, G.; Stoica, T.; Mantl, S.; Ikonic, Z.; Luysberg, M.; Chiussi, S.; Hartmann, J. M.; Sigg, H.; Faist, J.; Buca, D.; Grutzmacher, D. Lasing in direct-bandgap GeSn alloy grown on Si. *Nat. Phot.* **2015,** 9, 88-92.

(6) Homewood, K. P.; Lourenco, M. A. The rise of the GeSn laser. *Nat. Phot.* **2015,** 9, 78-79.

(7) Biswas, S.; Doherty, J.; Saladukha, D.; Ramasse, Q.; Majumdar, D.; Upmanyu, M.; Singha, A.; Ochalski, T.; Morris, M. A.; Holmes, J.D. Non-equilibrium induction of tin in germanium: towards direct bandgap $Ge_{1-x}Sn_x$ nanowires. *Nat. Comm.* **2016,** 7, 11405.

(8) Elbaz, A.; Buca, D.; von der Driesch, N.; Pantzas, K.; Patriarche, G.; Zerounian, N.; Herth, E.; Checoury, X.; Sauvage, S.; Sagnes, I.; Foti, A., Ossikovski, R.; Hartmann, J. M.; Boeuf, F.; Ikonic, Z.; Boucaud, P.; Grutzmancher, D.; El Kurdi, M. Ultra-low-threshold continuous-wave and pulsed lasing in tensile-strained GeSn alloys. *Nat. Phot.* **2020**, 14, 375-382.

(9) Senaratne, C. L.; Wallace, P. M.; Gallagher, J. D.; Sims, P. E.; Kouvetakis, J.; Menendez, J. Direct gap $Ge_{1-y}Sn_y$ alloys: Fabrication and design of mid-IR photodiodes. *J. Appl. Phys.* **2016,** 120, 025701.

(10) Massalski, T.;Binary Alloy Phase diagrams, 2nd ed.; Massal-

ski, T., Ed.; ASM: Ohio, 1990; Vol. 2.

(11) Guillaume, C.; Serghiou, G.; Thomson, A.; Morniroli, J. P.; Frost, D. J.; Odling, N.; Mezouar, M. Tuning between Mixing and Reactivity in the Ge-Sn System Using Pressure and Temperature. *J. Am. Chem. Soc.* **2009,** 131, 7550-7551.

(12) Serghiou, G.; Guillaume, C. L.; Jeffree, C. E.; Thomson, A.; Frost, D. J.; Morniroli, J. P.; Odling, N. Imaging of mixing and reaction in group IV systems recovered from high pressures and temperatures. *High Pressure Res.* **2010,** 30, 44-50.

(13) Guillaume, C. L.; Serghiou, G.; Thomson, A.; Morniroli, J. P.; Frost, D. J.; Odling, N.; Jeffree, C. E. *Inorg. Chem.* Correlation between Structural and Semiconductor Metal Changes and Extreme Conditions Materials Chemistry in Ge-Sn **2010,** 49, 8230-8236.

(14) Serghiou, G.; Reichmann, H. J.; Odling, N.; Spektor, K.; Pakhomova, A., Crichton, W.; Konôpková, Z. An unexpected cubic symmetry in group IV alloys prepared using pressure and temperature *Angew. Chem. Ed.* **2021**, 60, 9009-9014.

(15) Young, D. A. Phase Diagrams of the Elements, 1st ed.; University of California Press: Berkeley, CA, 1991.

(16) Mujica, A.; Rubio, A.; Munoz, A.; Needs, R. J. High pressure phases of group IV, III-V, and II-VI compounds. *Rev. Mod. Phys.* **2003,** 75, 863-912.

(17) Hume-Rothery W.; Smallman, R. E. The Structure of Metals and Alloys,5th ed.; The Chaucer Press: London, 1969.

(18) Supporting information

(19) Wang, H.; Liu, J. F.; He, Y.; Wang, Y.; Chen, W.; Jiang, J. Z.; Staun Olsen, J. High-pressure structural behaviour of nanocrystalline Ge. *J. Phys. Cond. Matter*, **2007**, 19, 1-10.

(20) Di Cicco, A.; Frasini, A. C.; Minicucci, M.; Principi, E.; Itie, J. P.; Munsch, P. High-pressure and high-temperature study of phase transitions in solid germanium *Phys. Status Solidi B* **2003,** 240, 19-28.

(21) Cavaleri, M. E.; Plymate, T. G.; Stout, J. H. A pressure volume temperature equation of state for Sn(beta) by energy dispersive X-ray diffraction in a heated diamond-anvil cell. *J. Phys. Chem. Solids* **1988,** 49, 945-956.

(22) Plymate, T. G.; Stout, J. H.; Cavaleri, M. E. Pressure volume temperature behavior and heterogeneous equilibria of the non-quenchable body-centered tetragonal polymorph of metallic tin. *J. Phys. Chem. Solids*, **1988,** 49, 1339-1348.

(23) Salamat, A.; Briggs, R.; Bouvier, P.; Petitgirard, S.; Dewaele, A.; Cutler, M. E.; Cora, F.; Daisenberger, D.; Garbarino, G.; McMillan, P. F. High-pressure structural transformations of Sn up to 138 GPa: Angle-dispersive synchrotron x-ray diffraction study. *Phys Rev. B* **2013**, 88, 104104.

(24) Katzke, H.; Bismayer, U.; Toledano, P. Theory of the high pressure structural phase transitions in Si, Ge, Sn and Pb. *Phys. Rev. B* **2006,** 73, 134105.

(25) Christensen, N. E.; Methfessel, M. Density-functional calculations of the structural properties of tin under pressure. *Phys. Rev. B* **1993**, 48, 5797-5807.

(26) Fadaly, E. M. T.; Dijkstra, A.; Suckert, J. R.; Ziss, D.; van Tilburgh, M. A. J. A.; Marvin, J.; Mao, C. Y.; Ren, Y. Z.; van Lange, V. T.; Korzun, K.; Kolling, S.; Verheijen, M. A.; Busse, D.; Roedel, C.; Furthmueller, J.; Bechstedt, F.; Stangl, J.; Finley, J. J.; Botti, S.; Haverkort, J. E. M.; Bakkers, E. P. A. M. Direct-bandgap emission from hexagonal Ge and SiGe alloys. *Nature* **2020**, 580, 205-209.

(27) Oses, C.; Toher, C.; Curtarolo, S. High-entropy ceramics. *Nature Reviews Materials* **2020**, 5, 295-309.

(28) Xu, C.; Senaratne, C. L.; Kouvetakis, J.; Menendez, J. Compositional dependence of optical interband transition energies in GeSn and GeSiSn alloys. *Solid-State Electronics* **2015**, 110, 76-82.

(29) Manzoor, A.; Pandey, S.; Chakraborty, D.; Phillpot, S. R.; Aidhy, D. S. Entropy contributions to phase stability in binary random solid solutions. *npj Computational Materials* **2018**, 47, 1-10.

(30) Dragoe, N.; Berardan, D. Order emerging from disorder. *Science* **2019,** 366, 573-574.

(31) Li, R.; Liu, J.; Popov, D.; Park, C.; Meng, Y.; Shen, G. Experimental observations of large changes in electron density distributions in β-Ge. *Physical Review B* **2019**, 100, 224106.

Table of Contents Artwork